Journal of Engineering Science and Technology
Vol. 9, No. 2 (2014) 220 - 232

PRESSURE AND VELOCITY AMPLITUDES OF THE INCOMPRESSIBLE FLUID IN CONCENTRIC ANNULAR PASSAGE WITH OSCILLATORY BOUNDARY: TURBULENT FLOW

ABOLGHASEM MEKANIK, MOHAMAD ALI YAVARI*

Department of Mechanical Engineering, Bu-Ali Sina University, Hamadan, Iran
*Corresponding Author: mohamadaliv121@yahoo.com

Abstract

An unsteady program based on a turbulence model called Baseline (BSL) *k*-omega model was conducted to simulate three turbulent flows with Re numbers of 4×10^3, 8×10^3 and 1×10^4, between two initially concentric cylinders. The effects of principal flow variables, i.e., mean axial velocity and fluid temperature, annular passage configurations, i.e., the gap width and radii of cylinders on the pressure and circumferential velocity of a three dimensional turbulent flow in the annular passage were investigated. The results were validated with the available solutions in the literature and fairly good agreements are seen. By increasing the gap of the annular passage and the axial flow velocity, smaller values for the unsteady pressure and the circumferential velocity amplitudes are produced. For each of the turbulent flows the unsteady pressure amplitude increases with the fluid temperature, as well as the circumferential velocity amplitude. The results of this investigation are favorably used for FIV and FSI calculations in such configurations.

Keywords: Annular flow, Unsteady pressure and velocity, Oscillatory boundary, FIV, FSI.

1. Introduction

Many industrial and engineering structures are associated with internal, external or annular flows, especially those involving nuclear reactors, power generation and petroleum extraction. One of the geometries that are of great interest among scientists and researchers in this field, is the annular flow between two concentric cylinders; for instance control rods in guide tubes, feedwater spargers and fuel strings in coolant channels, in different types of nuclear reactors; oil conveying

Nomenclature

C	Damping coefficient, N.s/m
D	Diameter, m
F	Force, N
h	Gap width, m
K	Effective stiffness, N/m
M	Mass, kg
p	Pressure, Pa
r	Radial space component, m
T	Absolute temperature, K
t	Time, s
U	Reference velocity, m/s
u	Axial velocity component, m/s
$\mathbf{V}$	Velocity vector
v	Radial velocity component, m/s
w	Circumferential velocity component, m/s
x	Axial coordinate of space, m
y	Vertical coordinate of space, m

Greek Symbols

ε	Initial amplitude of oscillation, m
θ	Circumferential coordinate of space, deg.
ρ	Fluid density, kg/m^3
υ	Kinematic viscosity, m^2/s
ω	Frequency, Hz
∇	Divergence

Abbreviations

FIV	Flow-Induced Vibration
FSI	Fluid-Structure Interaction
MP	Mean position
Re	Reynolds Number
TDCT	Time-dependent coordinate transformation

Subscripts

D	Diameter
h	Hydraulic
i	Inner
Int	Interaction
o	Outer
∞	Downstream

and gas production systems in petroleum sites. A comprehensive list of such practical cases of annular flow-induced problems can be found in [1, 2].

The first explanation for the mechanism underlying annular-flow-induced instabilities is given by Miller [3] and the problem was studied further by Mulcahy [4] calculating the fluid forces exerted on rods vibrating in annular

regions. The first attempts to generate an analytical viscous model for the cylindrical geometry are due to Hobson [5] and Spurr and Hobson [6]. Several approaches have been used by different researchers to obtain theoretical or experimental studies on fluid-structure interactions in annular and leakage flows among them are Ashurts and Durst [7], Parkin and Watson [8], Mulcahy [9], Perotin [10] and Karagiozis et al. [11].

A more rigorous, purely analytical potential flow model was formulated by Mateescu & Paidoussis [12] for a rigid centre-body hinged at one point and coaxially positioned in a flow-carrying conduit. This rigid-body model was then extended to take into account viscous effects [13]. One of the principal findings of this work was that viscous effects stabilize the system, and that they become more important as the annulus becomes narrower. Further development in this area has been achieved by the use of computational models which involve simultaneous numerical integration of the Navier-Stokes equations for laminar flow, and the equation of motion of the structure [14]. One such attempt was made by Mateescu et al. [15,16], who used a computational method to integrate the linearized Navier–Stokes equations for small amplitude oscillations of the outer cylinder. A new formulation for unsteady annular flows based on a time-dependent coordinate transformation (TDCT), capable of solving accurately both cases of large and small amplitude oscillations of the solid boundaries was presented by Mateescu et al. [17]. A series of accurate experimental measurements of the unsteady pressure in the annulus between two concentric cylinders and the solution of the unsteady Navier–Stokes and continuity equations for the same annular geometry were conducted by Mekanik and Paidoussis to compare the experimental results with the theoretical ones [18].

Although a large number of studies have been carried out on the turbulent flow in annular passages, these works are in minority compared with those done on laminar flow. Moreover, the researches interested in turbulent annular flow have not taken all the effective variables into account. Hence there is a real need for more through studies on turbulent annular flow and its fluctuations due to changes in effective variables. The present work has used an unsteady program based on a turbulence model called Baseline (BSL) *k*-omega model to investigate the effects of principal flow variables and annular passage configurations on the unsteady pressure and circumferential velocity of a three dimensional turbulent flow in the annular passage between two initially concentric cylinders.

2. Method of Solution

2.1. Problem definition and theory

The annular passage conducting incompressible flow is formed of two initially concentric cylinders, one of which is mounted flexibly and free to experience transverse translational oscillations. In this study it is the outer cylinder which executes transverse vibrations, while the center body is fixed without any movement and the configuration of such system can be seen in Fig. 1.

The purpose of this work is to examine the effects of principal flow variables such as the axial velocity and fluid temperature and the annular configurations like gap width and radii of cylinders, on the unsteady pressure and the circumferential

velocity of flowing fluid in the three dimensional annular passage. An accurate analysis of the unsteady flows in the case of larger amplitudes of oscillation is important for the study of the dynamics of fluid-elastic systems beyond the first loss of stability, which is not only of academic, but also of practical interest. The results of the present work provide the engineers with raw material for designing a secure and robust structure based on the knowledge of pressure, circumferential velocity and consequently the amplitude of oscillations of the outer cylinder, which is the key indicator of threshold of fluid-elastic instabilities.

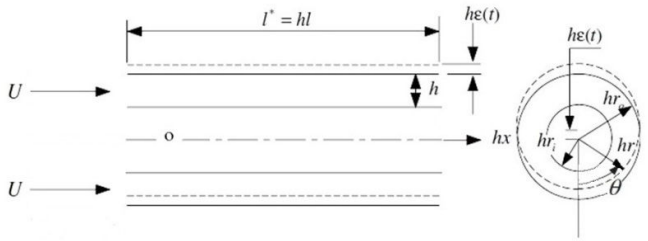

Fig. 1. Geometrical Representation of the Annular Passage.

As the first step to begin with, the outer cylinder is replaced from its initial position by a small magnitude, ε, and the problem is solved in steady state condition to obtain the flow field. Afterward, the outer cylinder is released to execute transverse vibrations and the fluid forces are generated which interact with the structure; the generated steady solution in the previous step is used as the initial conditions for the pressure and velocity throughout the fluid domain. An unsteady program was employed to simulate the three dimensional flow through annular passage and to predict the dynamical behavior of the oscillating tube in order to examine the course at which the flow quantities such as the unsteady pressure and unsteady circumferential velocity are produced.

In this study, the quantities with an asterisk are dimensional and according to Eq. (1) they are associated with their plain dimensionless counterparts, e.g. r_i^* and r_i; U, h and T which respectively represent mean axial velocity, gap width of annular space and fluid temperature are exceptionally dimensional. The radius of the inner cylinder is $r_i^*=hr_i$; thus the outer cylinder radius is $r_o^*=hr_o=hr_i+h$.

$$\begin{aligned} &x = x^*/h\,, \quad r = r^*/h\,, \quad \varepsilon = \varepsilon^*/h \\ &u = u^*/U\,, \quad v = v^*/U\,, \quad w = w^*/U \\ &p = (p^* - p_\infty^*)/(\rho^* U^2)\,, \quad \omega = \omega^* h/U \end{aligned} \tag{1}$$

where ε^* is the initial amplitude of oscillation, p^* the pressure, ρ^* the fluid density, ω^* the frequency of vibration, and u^*, v^* and w^* represent the velocity components in the axial, radial, and circumferential directions respectively.

In this investigation, the viscosity and density are assumed to remain constant unless stated otherwise. Thus, the continuity and Navier–Stokes equations, without body forces, are expressed in non-dimensional form as

$$\nabla.\mathbf{V} = 0 \tag{2}$$

$$\frac{\partial \mathbf{V}}{\partial t} + \nabla.(\mathbf{V}\,\mathbf{V}) = -\nabla p + \frac{2}{\mathrm{Re}_{D_h}}\nabla^2\mathbf{V} \tag{3}$$

where the Reynolds number in annular flow is defined in the following equation based on the hydraulic diameter of $D_h = 2h$,

$$\mathrm{Re}_{D_h} = 2hU/\upsilon^* \tag{4}$$

The program expanded to take the turbulence effects into account and examine the three dimensional turbulent flow in the annular passage, which is the main objective of the present fluid–structure interaction problem. To this end, a rigorous turbulence model called Baseline (BSL) *k*-Omega Model is used which is a combination between the k-ω model near the surface and the k-ε model in the outer region of the flow. The blending will take place in the wake region of the boundary layer. This model consists of a transformation of the k-ε model to a k-ω formulation and a subsequent addition of the corresponding equations. The difference between this formulation and the original k-ω model is that an additional cross-diffusion term appears in the ω-equation and that the modeling constants are different [20]. A second order backward Euler scheme is used to solve equations in transient simulations.

After solving the Navier-Stokes and continuity equations simultaneously and evaluating the unsteady fluid force exerted on the oscillating outer cylinder, the equation of motion of the outer cylinder, Eq. (5), is solved to determine the unsteady displacement of the outer tube;

$$M\ddot{y} + C\dot{y} + Ky = F_{Int} \tag{5}$$

where M is the mass, K the effective stiffness, C the damping coefficient of the structure and F_{Int} the unsteady fluid force. All the flow field variables change periodically due to harmonic motion of outer cylinder; hence they possess a periodic nature and consist of the steady plus the complex unsteady component. A Fourier transform has been used to extract the amplitude and phase angle of unsteady the flow quantities with respect to the displacement of the outer cylinder.

2.2. Boundary conditions and mesh survey

Based on what mentioned earlier one can deduce that the flow characteristics, annular passage configurations and the outer cylinder motion are symmetric with respect to the vertical plane positioned at $\theta=0$, as shown in Fig. 1; therefore it is possible to simulate the problem for the half of the geometry without losing the accuracy of the solution while saving the time of computation. In this case the problem contains five boundary conditions including inlet, outlet, inner tube, outer tube and symmetry. The inner tube is fixed but the outer cylinder is flexibly supported and its translational motion takes place in the given plane of symmetry. Hence the harmonic motion of the outer tube is defined by a numerical code derived from Eq. (5), i.e., the equation of motion of an object under forced vibration. However for the purpose of studying the effect of fluid damping on the structure, the structural damping C is neglected.

One of the most important steps is to generate a satisfactory grid which is fairly fine in mesh. In addition, in order to consider energy dissipation within the boundary layers adjacent to the walls, the mesh needs to be stretched near the cylinders. A comparative study between four meshes with different refinement was carried out to gain the solution independent of mesh refinement. Finally a structured

and near wall stretched mesh with 324800 elements was chosen which consists of 140 grid points in the x, 80 grid points in the θ and 29 grid points in the r direction.

2.3. Method validation

The comparison has been made between present results and an experimentally confirmed set of numerical results of Ref. [19]. Figures 2(a) and (b) show the amplitudes of non-dimensional unsteady pressure p and the corresponding phase angles with respect to the translational displacement of the outer cylinder versus axial coordinate of the cylinder in a uniform annular geometry for two sets of results. In reference [19] two different methods were used by the authors, MP (Mean Position) and TDCT (Time-dependent Coordinate Transformation) methods. TDCT results are more reliable for problems with larger oscillation amplitude. Figures 3(a) and (b) compare the present results with those of Ref. [19] for the unsteady amplitude of non-dimensional circumferential velocities w, and the corresponding phase angles. Although the outcome of the present simulation doesn't coincide exactly with the referred results, good almost agreement between the two groups of results indicates the precise simulation of the present work.

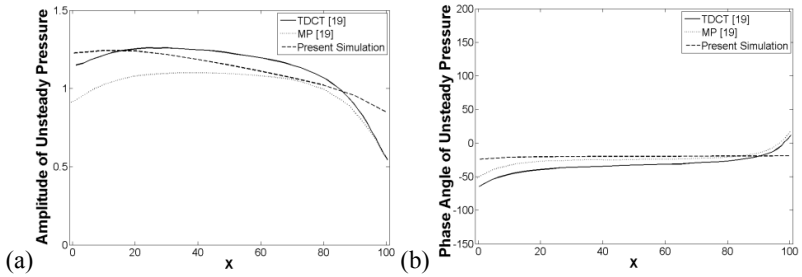

Fig. 2. (a) The Non-Dimensional Unsteady Pressure and (b) the Corresponding Phase Angle for $\mathrm{Re}_{D_h} = 250$, $\omega = 0.2$, $r_i = 9$, $r_o = 10$, $\varepsilon = 0.2$ at $r = 9.965$, $\theta = 7.5°$.

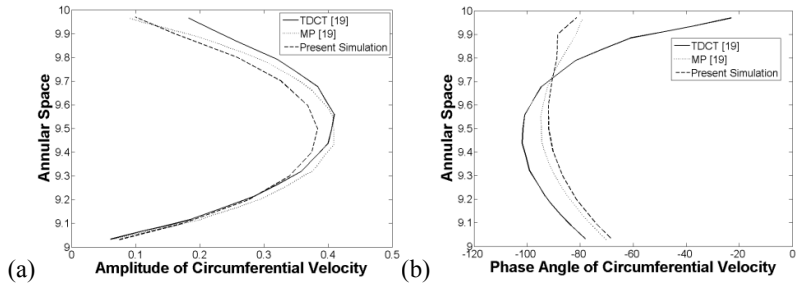

Fig. 3. (a) The Non-Dimensional Circumferential Velocity and (b) the Corresponding Phase Angle for $\mathrm{Re}_{D_h} = 250$, $\omega = 0.2$, $r_i = 9$, $r_o = 10$, $\varepsilon = 0.2$ at $x = 50$, $\theta = 45°$.

In this study three turbulent Reynolds numbers were selected to imply a proper collation of the flow quantities and to obtain an adequate perspective of turbulent annular flow. The chosen Reynolds numbers consist of 4×10^3, 8×10^3 and 1×10^4 which have been calculated using Eq. (4).

3. Results and Discussion

The 3D turbulent flow through annular passage with oscillating outer cylinder and fixed center body was simulated and the following results were obtained. First the effect of mean axial velocity, *U*, which is one of the important variables and determines the flow pattern, on the flow quantities was investigated and the results are presented in Figs. 4 and 5. As the axial flow velocity and subsequently the Reynolds number increases, the amplitude of the unsteady pressure decreases. Figure 4(a) shows that the amplitude of unsteady pressure in the first turbulent flow with Re = 4000 is considerably higher than the amplitudes of other turbulent flows. Figure 4(b) shows that the phase angles of the unsteady pressure at three investigated turbulent flows almost take negative values and decrease as the mean axial velocity increases. This trend shows that an increase in the reference velocity, *U*, will result in lower added damping which means that the solution of the present problem approaches to the potential flow solution, which is in agreement with the physics of the fluid mechanics problem.

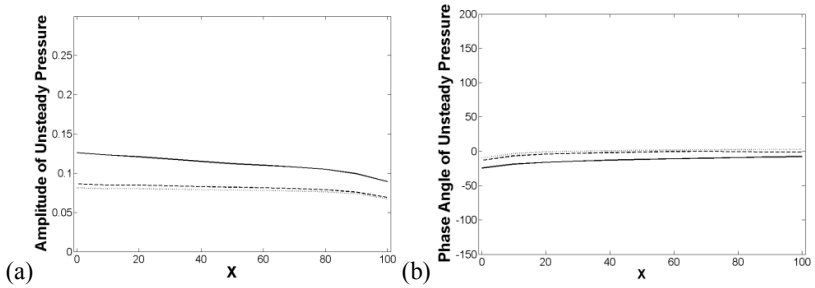

Fig. 4. (a) The Non-Dimensional Unsteady Pressure and (b) the Corresponding Phase Angle at $r=9.965$, $\theta=7.5°$ for $\omega=0.1$, $r_i=9$, $r_o=10$, $\varepsilon=0.1$; —— Re=4×10^3; – – – Re=8×10^3; ····· Re=1×10^4.

In Fig. 5 the amplitude of circumferential velocity in annular space and its phase angle with respect to the displacement of the outer cylinder is depicted. It can be seen that the amplitude of circumferential velocity decreases as the mean axial velocity increases. There is a sharp decline in the amplitude of the circumferential velocity while the mean axial velocity and subsequently the Reynolds number increases from 4000 to 8000 and then the circumferential velocity almost remains constant. As mentioned for the amplitude, the magnitude of the phase angle decreases as the Reynolds number increases from 4000 to 8000 and after that it doesn't experience any significant change.

Fluid hydrodynamic characteristics are intensely dependent on temperature and it is expected that the fluid dynamic behavior changes as its temperature varies. For a particular gas, a rise in temperature results in higher degree of

molecular movements and a larger dynamic viscosity; unlike the liquids that their viscosities decrease with an increase in temperature. In this case for each of turbulent flows, mean axial velocity remains constant when increasing the fluid temperature; thus according to Eq. (4) Reynolds numbers reduce to lower values in comparison to the earlier values. Figure 6(a) shows that for each turbulent flow the unsteady pressure amplitude increases with the fluid temperature. The increment of the pressure amplitude is not the same for three turbulent flows; the first turbulent flow with initial Reynolds number of 4000 gained the highest value of growth in the pressure amplitude, i.e., 16%, while the second flow has the lowest value, i.e., 9%. In Fig. 6(b) it is noticed that the magnitude of the phase angle of unsteady pressure increases as the fluid temperature goes up.

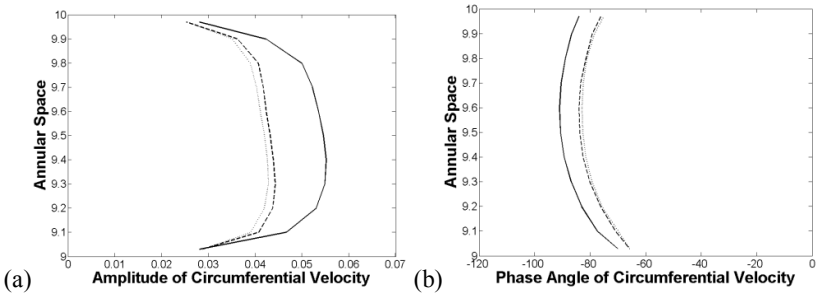

(a) (b)

Fig. 5. (a) The Non-Dimensional Circumferential Velocity and (b) the Corresponding Phase Angle at $x = 50$, $\theta = 45°$ for $\omega = 0.1$, $r_i = 9$, $r_o = 10$, $\varepsilon = 0.1$; —— Re=4×10^3; – – – Re=8×10^3; ····· Re=1×10^4.

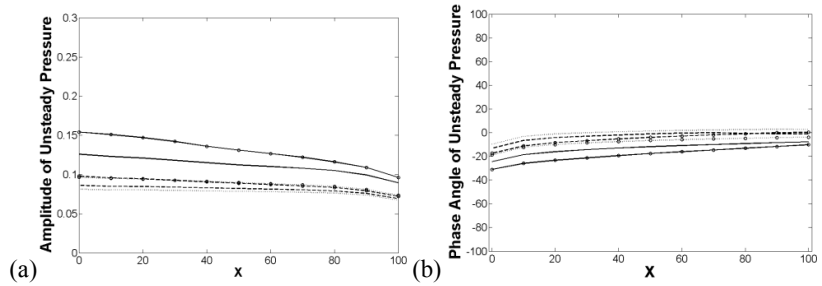

(a) (b)

Fig. 6. (a) The Non-Dimensional Unsteady Pressure and (b) the Corresponding Phase Angle at $r = 9.965$, $\theta = 7.5°$ for $\omega = 0.1$, $r_i = 9$, $r_o = 10$, $\varepsilon = 0.1$; —— Re=4×10^3, T=300 K; —o— Re=2386, T=400 K; – – – Re=8×10^3, T=300 K; –o– Re=4773, T=400 K; ····· Re=1×10^4, T=300 K, ··o··· Re=5966, T=400 K.

In Fig. 7(a) it can be seen that the value of the circumferential velocity amplitude increases with the fluid temperature. However, the change in the amplitude of circumferential velocity in the second turbulent flow doesn't seem to be noticeable. The third turbulent flow shows a substantial increase in circumferential velocity amplitude. According to Fig. 7(b), although the rise in fluid temperature of the first and second flows doesn't change the magnitude of

the circumferential velocity phase angle considerably, the magnitude of the phase angle in the third turbulent flow increases with the fluid temperature.

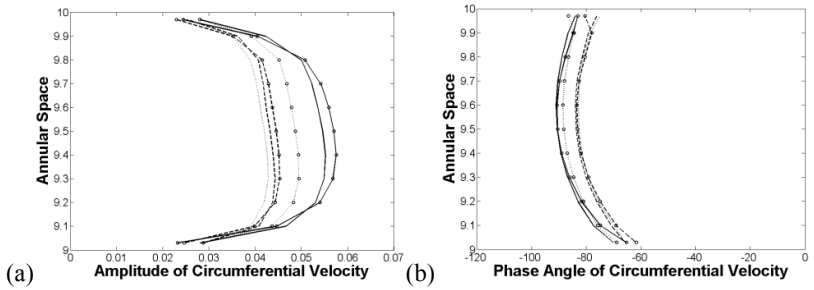

(a) (b)

Fig. 7. (a) The Non-Dimensional Circumferential Velocity and (b) the Corresponding Phase Angle at $x = 50$, $\theta = 45°$ for $\omega = 0.1$, $r_i = 9$, $r_o = 10$, $\varepsilon = 0.1$; —— Re=4×10^3, T=300 K; —o— Re=2386, T=400 K; – – – Re=8×10^3, T=300 K; –o– Re=4773, T =400 K; ····· Re=1×10^4, T=300 K; ··o··· Re=5966, T=400 K.

The gap width of the annular passage, h, plays an important role in the dynamics of the fluid flow through annuli. Two distinctive values designated for the annular passage gap width to investigate its effect on the unsteady pressure and the circumferential velocity of fluid, i.e., h = 1 and h = 2 cm. It can be seen in Fig. 8(a) that by increasing the gap of the annular passage, lower value for the unsteady pressure amplitude is produced. A set of calculations for the results obtained by the authors demonstrated that the mean unsteady pressure amplitudes of the new geometry are 21%, 46% and 51% smaller than those of the basic geometry for respectively the first, second and third Reynolds number. Figure 8(b) also shows a substantial increase in the magnitude of the phase angle of three turbulent flows as the gap width of the annular passage increases. The phase angles increments of the unsteady pressure approaches -90°, -50° and -41° for the first, second and third turbulent flows respectively. It is worthwhile noting that in the new geometry with larger annular space the structure gets larger added damping vis-à-vis the flow through basic geometry.

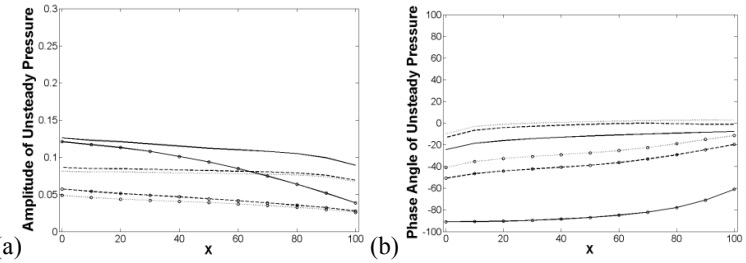

(a) (b)

Fig. 8. (a) The Non-Dimensional Unsteady Pressure and (b) the Corresponding Phase Angle at $r = 9.965$, $\theta = 7.5°$ for $\omega = 0.1$, $r_o = 10$, $\varepsilon = 0.1$; —— Re=4×10^3, h=1 cm; —o— Re=2386, h=2 cm; – – – Re=8×10^3, h=1 cm; –o– Re=4773, h=2 cm; ····· Re=1×10^4, h=1 cm; ··o··· Re=5966, h=2 cm.

Figures 9(a) and (b) represent the amplitude of the circumferential velocity and its phase angle with respect to the displacement of the outer cylinder versus two distinctive values of gap width. It is clearly seen in Fig. 9(a) that when the gap width doubles, the amplitude of circumferential velocity reduces. The present computational analysis shows that when the gap with, h, increases the maximum amplitudes of the circumferential velocity for the first, second and third turbulent flows decrease by 50, 41 and 36 percent respectively. The increase in the annular space also results in a larger phase angle for the circumferential velocity.

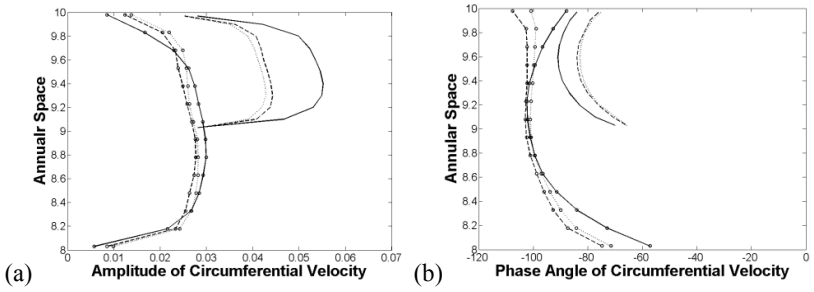

Fig. 9. (a) The Non-Dimensional Circumferential Velocity and (b) the Corresponding Phase angle at $x = 50$, $\theta = 45°$ for $\omega = 0.1$, $r_o = 10$, $\varepsilon = 0.1$; —— Re=4×10^3, h=1 cm; —o— Re=2386, h=2 cm; – – – Re=8×10^3, h=1 cm; –o– Re=4773, h=2 cm; ····· Re=1×10^4, h=1 cm; ···o··· Re=5966, h=2cm.

The effect of changing the radii of cylinders on the unsteady pressure and the circumferential velocity is investigated in this section. The values used for radii here are based on the non-dimensional radii used by Mekanik et al. [18]; hence the non-dimensional radii of the inner and outer cylinders changed to 4.785 and 5.785 respectively. The gap width of the annulus remains constant and one can conclude that the observed changes in flow behavior are purely due to the reduction of radii of cylinders. The amplitude of unsteady pressure and the corresponding phase angle with respect to the displacement of the outer cylinder is depicted in Figs. 10(a) and (b) for turbulent flows and two distinct geometries. The amplitudes of the unsteady pressure in the new geometry with smaller radii are clearly lower in comparison to those of the previous geometry. In the first turbulent flow with Reynolds number 4×10^3, the ratio of the mean unsteady pressure amplitude in the geometry with smaller radii to that of the previous geometry with larger radii is about 0.4 while this ratio decreases to 0.3 for the last turbulent flow with Reynolds number 1×10^4. In the new geometry, the phase angles of the unsteady pressure for turbulent flows are of larger magnitude with respect to the phase angles of basic geometry and as the Reynolds number increases the phase angles tend to zero, the same conclusion mentioned before with regards to approaching the potential flow when Reynolds number increases.

Figure 11 represents the amplitude of circumferential velocity and its phase angel with respect to the displacement of outer cylinder versus two different sets of radii of cylinders. It is clearly seen in Fig. 11(a) that the amplitude of circumferential velocity decreases with changes made in the radii of annulus.

More precisely the maximum value of the circumferential velocity in the three examined turbulent flows with Reynolds number 4×10^3, 8×10^3 and 1×10^4 decreases by 39%, 34% and 29% respectively as the radii of cylinders reduce. Figure 11(b) shows that larger magnitudes of phase angle are obtained in the new geometry with smaller radii.

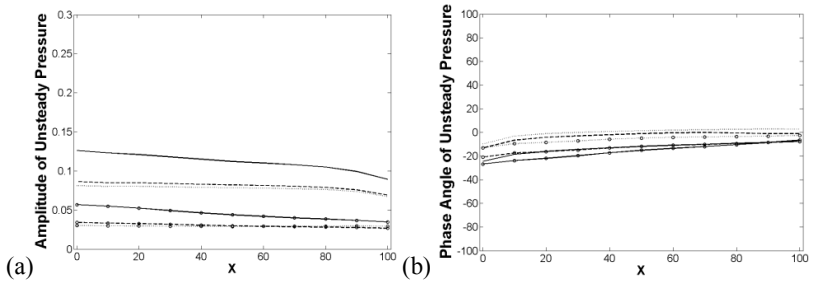

Fig. 10. (a) The Non-Dimensional Unsteady Pressure and (b) the Corresponding Phase Angle at $r = 9.965$ and 5.75, $\theta = 7.5°$ for $\omega = 0.1$, $\varepsilon = 0.1$; —— Re=4×10^3, $r_i = 9$, $r_o = 10$; —o— Re=4×10^3, $r_i = 4.785$, $r_o = 5.785$; – – – Re=8×10^3, $r_i = 9$, $r_o = 10$; –o– Re=8×10^3, $r_i = 4.785$, $r_o = 5.785$; ····· Re=1×10^4, $r_i = 9$, $r_o = 10$; ··o··· Re=1×10^4, $r_i = 4.785$, $r_o = 5.785$.

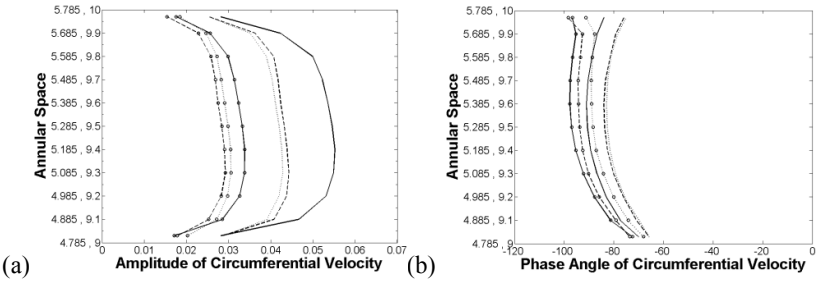

Fig. 11. (a) The Non-Dimensional Circumferential Velocity and (b) the Corresponding Phase Angle at $x = 50$, $\theta = 45°$ for $\omega = 0.1$, $\varepsilon = 0.1$; —— Re=4×10^3, $r_i = 9$, $r_o = 10$; —o— Re=4×10^3, $r_i = 4.785$, $r_o = 5.785$; – – – Re=8×10^3, $r_i = 9$, $r_o = 10$; –o– Re=8×10^3, $r_i = 4.785$, $r_o = 5.785$; ····· Re=1×10^4, $r_i = 9$, $r_o = 10$; ··o··· Re=1×10^4, $r_i = 4.785$, $r_o = 5.785$.

4. Conclusions

In the present work the effects of principal flow variables, as well as the annular configurations, on the circumferential velocity and the unsteady pressure of an incompressible fluid in the three dimensional annular passages were studied. It is concluded that as the axial flow velocity increases, the amplitudes of unsteady pressure, the circumferential velocity and the corresponding phase angles with respect to the displacement of the outer cylinder decrease. An increase in the reference velocity, *U*, results in lower added damping which means that the solution of the present problem tends to that of the potential flow. For each

turbulent flow the unsteady pressure amplitude increases with the fluid temperature, as well as the circumferential velocity amplitude. It is also noticed that the magnitude of the phase angle of the unsteady pressure increases as the fluid temperature goes up. By increasing the gap of the annular passage, lower values for the unsteady pressure and the circumferential velocity amplitudes are obtained. It is also noticed that a considerably higher added damping is achieved as the gap width between the two cylinders doubled. A new geometry built of cylinders with smaller radii was considered by the authors. The ratio of the mean unsteady pressure amplitude in the geometry with smaller radii to that of the previous geometry for the first turbulent flow with Reynolds number 4×10^3 is about 0.4 while this ratio decreases to 0.3 for the last turbulent flow with Reynolds number 1×10^4. The corresponding figures also illustrated that the amplitude of circumferential velocity decreases with the radii of annulus. Larger magnitudes of phase angles were obtained in the new geometry with smaller radii.

References

1. Paidoussis, M.P. (1998). *Fluid–structure interactions, slender structures and axial flow, Vol.* 1. London: Academic Press.
2. Paidoussis, M.P. (2003 *Fluid–structure interactions, slender structures and axial flow, vol.* 2. London: Elsevier Academic Press.
3. Miller, D.R. (1970). Generation of positive and negative damping with a flow restrictor in axial flow. *Proceedings of the Conference on Flow-Induced Vibrations in Reactor System Components*. Argonne National Laboratory Report ANL7685, Argonne IL, USA, 304-311.
4. Mulcahy, T.M. (1980). Fluid forces on rods vibrating in finite length annular regions. *ASME Journal of Applied Mechanics*, 47(2), 234-240.
5. Hobson, D.E. (1982). Fluid-elastic instabilities caused by flow in an annulus. *Proceedings of 3rd International Conference on Vibration of Nuclear Plant*, Keswick, UK. BNES, London, 460-463.
6. Spurr, A.; and Hobson, D.E. (1984). Forces on the vibrating center-body of an annular diffuser. *ASME Symposium on Flow-induced Vibration, Vibration Induced by Axial and Annular Flows*, Vol. 4, ASME, New York, 41-52.
7. Ashurts, W.T.; and Durst, F. (1980). *Studies of flow instabilities in two dimensional test sections with sudden expansions, practical experiences with flow-induced vibrations*. Naudascher, E.; and Rockwell, D. (Eds.), 801-808.
8. Parkin, M.W.; and Watson, C.P. (1984). Reduction of vibration caused by flow in an annular diffuser. *ASME symposium on flow-induced vibration*, Vol. 4: Vibration induced by axial and annular flows, Paidoussis, M.P.; and Au-Yang, M.K. (Eds.), 1-14.
9. Mulcahy, T.M. (1988). One-dimensional leakage-flow vibration instabilities. *Journal of Fluids and Structures*, 2(4), 383-403.
10. Perotin, L. (1994). Fluid-structure coupling between a vibrating cylinder and a narrow annular flow. *Nuclear Engineering and Design*, 149(1-3), 279-289.
11. Karagiozis, K.N.; Paidoussis, M.P.; Amabili, M.; and Misra, A.K. (2008). Nonlinear stability of cylindrical shells subjected to axial flow: Theory and experiments. *Journal of Sound and Vibration*, 309(3-5), 637-676.

12. Mateescu, D.; and Paidoussis, M.P. (1985). The unsteady potential flow in an axially-variable annulus and its effect on the dynamics of the oscillating rigid center-body. *ASME Journal of Fluids Engineering*, 107(2), 413-427.
13. Mateescu, D.; and Paidoussis, M.P. (1987). Unsteady viscous effects on the annular-flow-induced instabilities of a rigid cylindrical body in a narrow duct. *Journal of Fluids and Structures*, 1(2), 197-215.
14. Paidoussis, M.P.; Mateescu, D.; and Belanger, F. (1992). A computational method for the dynamics of cylindrical structures subjected to annular flows by simultaneous integration of the Navier-Stokes and structural equations. *International Symposium on Flow-Induced Vibration and Noise: Axial and Annular Flow-Induced Vibration and Instabilities*, Vol. 5, ASME, New York, 17-32.
15. Mateescu, D.; Paidoussis, M.P.; and Belanger, F. (1994). A time-integration method using artificial compressibility for unsteady viscous flows. *Journal of Sound and Vibration*, 177(2), 197-205.
16. Mateescu, D.; Paidoussis, M.P.; and Belanger, F. (1994). Unsteady annular viscous flows between oscillating cylinders. Part I: computational solutions based on a time integration method. Part II: a hybrid time-integration solution based on azimuthal Fourier expansions for configurations with annular backsteps. *Journal of Fluids and Structures*, 8(5), 489-507 and 509-527.
17. Mateescu D., Mekanik A., Paidoussis, M.P. (1996). Analysis of 2-D and 3-D unsteady annular flows with oscillating boundaries based on a time-dependent coordinate transformation. *Journal of Fluids and Structures*, 10(1) 57-77.
18. Mekanik, A.; and Paidoussis, M.P. (2007). Unsteady pressure in the annular flow between two concentric cylinders one of which is oscillating: Experiment and theory. *Journal of Fluids and Structures*, 23(7), 1029-1046.
19. Mekanik, A.; and Paidoussis, M.P. (2007). Stability analysis of uniform and non-uniform annular passages conducting incompressible laminar flows for small and large amplitude oscillatory motions of the outer cylinder. *Journal of Sound and Vibration*, 303(1-2), 78-108.
20. Menter. F.R. (1994). Two-equation eddy-viscosity turbulence models for engineering applications. *AIAA Journal*, 32(8), 1598-1605.